Journal of Magnetics 16(3), 206-210 (2011) http://dx.doi.org/10.4283/JMAG.2011.16.3.206

Optimization of Ferromagnetic Resonance Spectra Measuring Procedure for Accurate Gilbert Damping Parameter in Magnetic Thin Films Using a Vector Network Analyzer

D.-H. Kim[1], H.-H. Kim[1], Chun-Yeol You[1]*, and Hyungsuk Kim[2]*

[1]Department of Physics, Inha University, Namgu Incheon 402-751, Korea
[2]Department of Electrical Engineering, Kwangwoon University, Seoul 139-701, Korea

(Received 17 May 2011, Received in final form 3 Augut 2011, Accepted 4 August 2011)

We optimize a vector network analyzer ferromagnetic resonance (VNA-FMR) measurement system to study spin dynamics and Gilbert damping parameters of thin ferromagnetic films. In order to obtain accurate damping parameters, careful determination of the susceptibility line-width is required. The measured S-parameters are converted into the corresponding susceptibility through a calibration processes. From the line-width measurements, we can successfully extract the saturation magnetizations and Gilbert damping parameters of 5-, 8-, and 10-nm thick $Ni_{81}Fe_{19}$ (Py) films.

Keywords: Gilbert damping parameter, vector network analyzer, Kittel's equation, susceptibility

1. Introduction

There has been a large amount of research into the development and study of information-storage devices over a range of fields [1]. Although this research has greatly advanced, the demand for storage capacity always overwhelms the speed of research and development. A great variety of research has been performed to overcome this problems; much of this research has been associated with modern spintronic devices, including spin transfer torque (STT) magnetoresistive random access memory (MRAM) [2], race-track memory [3, 4], spin-torque nano-oscillators [5], non-uniform magnetic field induced domain wall memory [6], and domain wall MRAM [7]. The performance of these devices is related to their Gilbert damping parameter. In other words, it is important to measure the exact damping parameters of the ferromagnetic materials that are fundamental to the details of the spin dynamics in various spin devices.

In many experimental studiesa physically-meaningful analysis process for extracting the Gilbert damping parameter was not used, this usually leads to the assumption that the scattering parameter is proportional to magnetic susceptibility. In order to get more detailed information about the damping parameter, we need not only a well-organized, accurate measuring tool but also a well-defined, theory based process. Fortunately, recently this was provided by a well organized analysis in C. Bilzer's thesis [8]. We apply these procedures and techniques to obtain the damping parameter, which is characterized by a ferromagnetic resonance line-width as a function of the external magnetic field.

There has been a lot of measurement techniques developed for measuring the magnetic dynamic damping parameter. One of the first methods was pulse inductive microwave magnetometery (PIMM). PIMM is similar to a vector network analyzer ferromagnetic resonance setup, but it operates in a time domain. Although the frequency range is unlimited in principle, the pulse generator needs to be capable to producing a pulse shape that contains a corresponding high frequency component, this often leads to a low pumping efficiency for the respective frequency [9]. Other methods use the ferromagnetic resonance (FMR) phenomena. Generally FMR refers to an energy-absorption mechanism in the precession motion of the magnetization in a ferromagnetic material. More specifically, if an external magnetic field is applied, the magnetization precesses around the field direction. And then if the sample is irradiated with a transverse RF field and the RF frequency coincides with the precession frequency, the re-

*Co-corresponding authors: Tel: 82-32-860-7667
Fax: +82-32-872-7562, e-mail: cyyou@inha.ac.kr;
Tel: +82-2-940-8373, Fax: +82-2-940-5141, e-mail: hskim@kw.ac.kr

sonance condition is fulfilled and the microwave power is effectively absorbed by the ferromagnetic substance. Using this effect, there are two well-known methods of FMR measurement. Conventional ferromagnetic resonance (C-FMR) sweeps the external magnetic field H_{ext} with a small RF magnetic field with fixed frequency [10]. However, there are some problems with this measurement technique: H_{ext} disturbs the domain structure and it requires a larg sample size [11]. The other method uses a tool called a vector network analyzer ferromagnetic resonance (VNA-FMR). By using a VNA-FMR, we can adjust the microwave frequency as well as H_{ext}. This makes it possible to investigate a magnetic system in thin films without changing H_{ext}- the fixed external field. Although the frequency range is limited by the network analyzer's specification, dynamic properties of the magnetic system studied in any fixed field allow a dynamic response from the specific domain configurations in the magnetization of sample. For example, the absorption as a function of frequency provides us the response to the external RF magnetic field of a given sample. Then, we can use the appropriate data analysis from wave transmission geometry, where a rigorous analysis is possible [8].

In following section, we first introduce the measurement system more specifically and explain the calibration process, which uses a calibration kit containing a coplanar waveguide. Secondly, we explain the evaluation method for converting from a scattering parameter to susceptibility to find an accurate line-width. Then, we describe the experimental results from the VNA-FMR data at various thickness of $Ni_{81}Fe_{19}$ (Py). Finally, we obtain the Gilbert damping parameter and saturation magnetization M_s from the line-width and resonance frequency of the FMR spectra. In this study we explain a measurement system and process and show the signal/noise enhancement in this system compared with the previous results [12, 13]. Finally, we apply an appropriate experimental process to look at a Py sample series.

2. Measurement System and Basic Theory

We used a VNA (HP 8510C with 8517A option), which has frequency range from 45 MHz to 50 GHz for FMR measurements. A coplanar waveguide (CPW) is used with a Cascade Microtech impedance standard substrate GSG (ground-signal-ground), shaped open-strip line [14]. We also use a probe tip, GGB Industries 40M-GSG-100-PLL model (100 μm pitch and matched 50 Ω and made with non-magnetic material) [15]. The DC electromagnet has maximum field of 1 T, and the magnet system can be rotated through 360°. It is useful to derive the reference signal by applying a DC magnetic field, called external magnetic field, parallel to the direction of the RF magnetic field. In an additional rotation system is useful for setting the background signal; as mentioned in the previous section, there is no FMR when H_{ext}'s direction is parallel to H_{RF}'s. To remove and compensate for the noise from cable contact, we calibrate the probe using a calibration kit composed of an open, short, and load before the experimental process [16]. The schematic of theses processes is shown in Fig. 1: Short (short-circuit) means the signal line is connected with ground (GND), Open (open-circuit) is disconnected between the signal line and GND, and Load consist of a resistance material (matching 50 Ω) between the signal line and GND using up energy in this portion. Each part is in contact with the probe as shown in Fig. 1. These three parts are very important to the process before taking the measurement. In other words, any unwanted outside effects are eliminated by the calibration step. Then, the CPW, which has an impedance of 50 Ω, is placed in contact with the probe, and a ferromagnetic film is loaded onto the CPW. Finally, as can be seen in Fig. 2, we apply a DC magnetic field parallel to (*x*-direction) the CPW. To make a RF field in the perpendicular direction (*y*-direction), an AC current source is applied in the parallel direction (*x*-direction). To understate this mechanism, a schematic of the measurement system is sketched in Fig. 2. It is contained within the vector network analyzer (VNA) and coplanar waveguide (CPW). Resonance phenomena appear when the external field, H_{ext}, represented by a pink arrow is parallel to the CPW's GSG lines. The RF field, H_{RF}, represented by a blue arrow is perpendicular to the H_{ext}'s direction in the same plane (*x*-*y* plane).

More specifically when H_{ext} is applied, the magnetic moment precesses around the direction of H_{ext} (*x*-axis) at its frequency. Although the precession motion is affected by the effective field, given by $H_{eff} = H_{ext} + H_{uni} + H_{ex}$ where H_{ani} and H_{ex} are anisotropy and exchange fields,

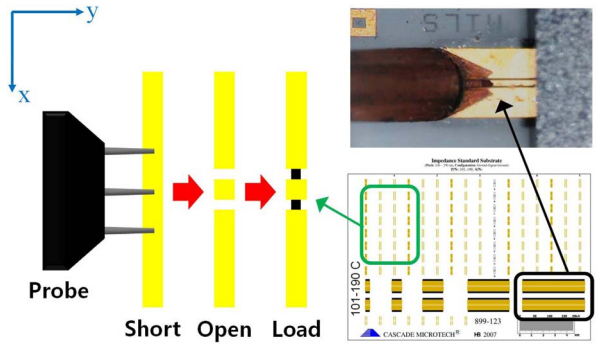

Fig. 1. (Color online) The process of calibration containing short, open and load in the CPW.

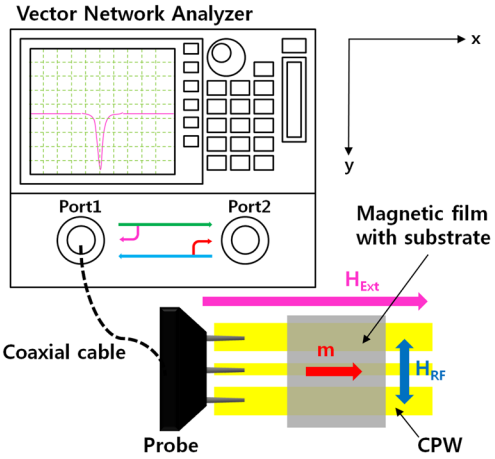

Fig. 2. (Color online) Schematic of the VNA-FMR measurement system: The sample is placed on the coplanar waveguide as indicated on the lower right hand side connected probe and coaxial cable, where the static H_{ext} is perpendicular to the excitation pulse H_{RF}.

H_{ext} dominates when the other parts are small in the Landau-Lifshitz equation. In this case, when the AC current flows in the signal line H_{RF} appears to also contain RF-frequency. By coincidence, if the two frequencies are the same, resonance phenomena, including energy abortion, exist. This is concept of the FMR mechanism.

After measuring the sample, we obtained scattering parameter (S-parameter) correlations between the incident and reflected electromagnetic waves. More specifically, S_{ij} represents the ratio of the outgoing wave at port i to the incident wave at port j. For example, S_{11} is the value from source out of one-port reflecting into itself, which is represented by a complex value.

S-parameters are related by susceptibility χ explaining the magnetic properties. There are well-described methods to obtain χ from the S-parameters. The first one of these is a two-port probe measurement, connected by two high-frequency probes to the VNA [17]. The sample is placed on the CPW between and in contact with the probes and, in this geometry, the distance from probe contact point to the sample position relative to the CPW plays an important role in determination of the S-parameters. To eliminate this dependence, new parameters are used to be revised by S_{11}, S_{21}, and S_{22}. Then χ can be simply expressed by this process. Another method uses one-port measurement with an open circuit CPW [18]. Compared with the two-port measurement technique, it is considered to have a simplified calibration and produces faster measurements. In one port system, composed open circuit CPW, χ also appears more simple expression by S_{11}^R than that of two-port process: the expression is

$$X = \frac{\ln S_{11}^R}{\ln S_{11,\mathrm{ref}}^R} - 1 . \quad (1)$$

Where X is proportional to the susceptibility and S_{11}^R and $S_{11,\mathrm{ref}}^R$ are acquired by FMR measurement spectra of the sample and reference. These two methods look quite different but show similar results, using the same CPW as for the two-port measurement process. Actually, in the one-port measurement, the second unconnected port is set-up as an open-circuit. It uses only a single microwave probe which has the advantage of simplifying the calibration speeding up the process in comparison with a full two port calibration. For these reasons we use the one-port FMR spectra in our experiment.

3. Experimental Result and Discussion

We prepared a series of Cu/Py bilayers with various Py thicknesses. All samples are prepared under a low base pressure of 10^{-8} Torr with 1.5 mTorr Ar working gas pressure by the DC-magnetron sputtering. The deposition rates are 0.514 and 0.842 Å/s for the Py and Cu, respectively. Before the deposition, the Si substrates were cleaned with acetone, chloroform, and isopropyl alcohol. First, we deposit a 10-nm Cu layer, as the seed layer, on the top of the substrate at room temperature. After that, we deposit various thicknesses of Py, d_x (= 5, 8, and 10 nm), and a 5-nm Cu layer is deposited as a capping layers.

Before measuring the VNA-FMR spectra, hysteresis loops are measured using a vibrating sample magnetometer (VSM) and the results are depicted in Fig. 3 for the Cu/Py(d_x)/Cu samples. Since the coercivity of the ferromagnetic layer is very sensitive to its microstructure and surface roughness in addition to the anisotropy field, coercivities of slightly different thicknesses cause small changes, however, noticeable differences are not found. As we know, the magnetic moment is influenced by the amount of ferromagnetic substance, the magnetic moment is proportional to the Py layer's thickness between 5 and 10 nm as explained by Fig. 3.

In a previous study we performed we obtained a good signal in Py magnetic thin films of less than 10-nm to diminish noise from the FMR spectra background signal [12, 13]. There are many problems in this measurement system; for example deviation of magnetic pole causing a vibrating motion of the magnetic system, unstable CPW, non-optimization system settings, probes which contain magnetic material, and misunderstanding of analytic process to convert the S-parameter into the susceptibility. These factors have caused noise in FMR signal and distortion of the FMR resonance shape and have been widely

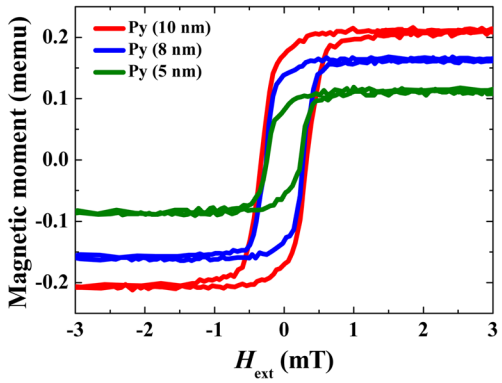

Fig. 3. (Color online) Hysteresis loops for various Py's thickness d_x in (a) Si/Cu(10 nm)/Py(10 nm)/Cu(5 nm), (b) Si/Cu(10 nm)/Py(8 nm)/Cu(5 nm), and (c) Si/Cu(10 nm)/Py(5 nm)/Cu(5 nm).

shown to occur in many research fields. We eliminate all these causes to obtain an improved signal which allows us to extract the exact Gilbert damping parameter.

We used VNA-FMR to measure the imaginary part of the χ of the sample. The measured raw data for the imaginary parts of the susceptibility is calibrated with careful calibration procedures. The calibrated imaginary parts of the χ are shown Fig. 4 for the sample Si/Cu(10 nm)/Py/Cu(5 nm) at a Py thickness of (a) 10 nm, (b) 8 nm, and (c) 5 nm in a frequency range from 4 to 12 GHz. The peaks of the spectra are moving with a magnetic field from 41 to 106 mT and the maximum intensity is declined as a function of $1/f_{res}$ in this range [8]. From Eq. (1) we can see this method and the well-made CPW calibration produce χ that is has a noticeably enhanced signal from the previous study [12, 13].

Next, from the FMR spectra, we found that the saturation magnetization M_s and Gilbert damping parameters α are extracted from the resonance frequency f_{res} and linewidth Δf. To obtain M_s, we use the resonance peaks which are well fitted with the Kittel's equation,

$$f_{res} = \frac{\gamma\mu_0}{2\pi}\sqrt{(H_{ext}+H_{uni})(H_{ext}+H_{uni}+M_s)}\,. \qquad (2)$$

Where, γ, μ_0, H_{ext}, and H_{uni} are the gyromagnetic ratio, magnetic permeability, external magnetic field, and uniaxial anisotropy field, respectively. f_{res} and H_{ext} are from experimental data and H_{uni} and M_s are deduced from the dispersion relation using Eq. (2). Fig. 5 shows the resonance peaks and fitted results together, and we obtain that M_s for d_x = 10, 8, and 5 nm are (a) 0.930 ± 0.002 T, (b) 0.931 ± 0.001 T, and (c) 0.810 ± 0.001 T, respectively. The variation of M_s is also small, as we desired.

Finally we discuss the determination of the Gilbert damping parameter *a*. The relation of Δf as a function of H_{ext} is shown in Fig. 6 for each d_x. The Δf is related as

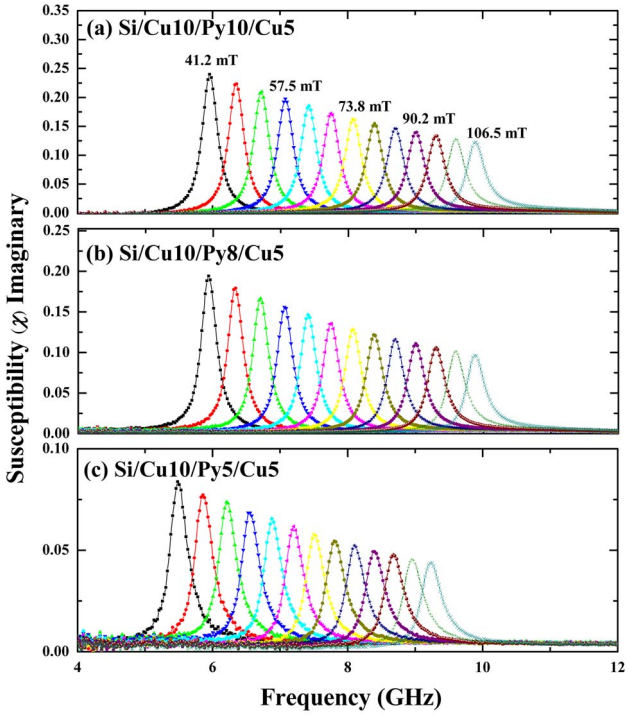

Fig. 4. (Color online) Imaginary parts of the susceptibility as a function of frequency with varied H_{ext} for various d_x (a) 10 nm, (b) 8 nm, and (c) 5 nm.

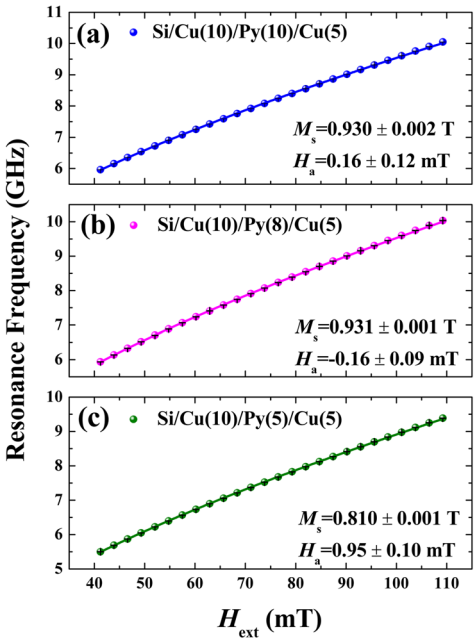

Fig. 5. (Color online) Resonance frequency as a function of field H_{ext} for various d_x (a) 10 nm, (b) 8 nm, and (c) 5 nm: symbols mean experimental data and solid lines are fitted results with the Kittel's equation.

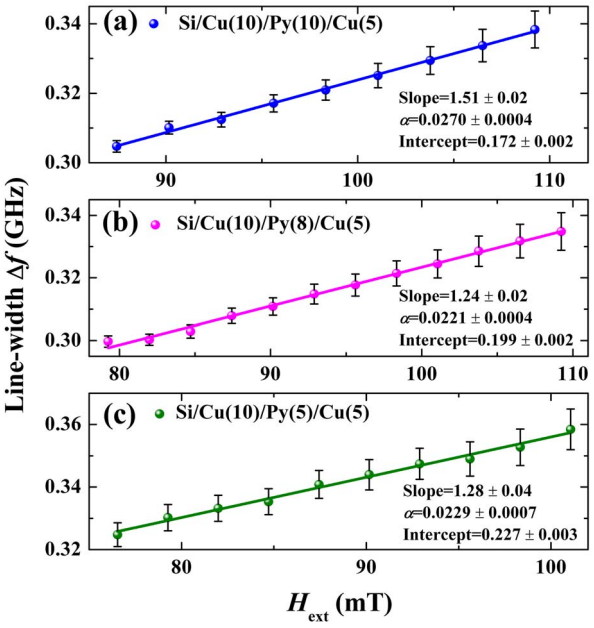

Fig. 6. (Color online) The line-width as a function of H_{ext}: symbols mean experimental data and solid lines are linear fitting for various d_x (a) 10 nm, (b) 8 nm, and (c) 5 nm.

follows:

$$\Delta f = \alpha\frac{\gamma\mu_0}{2\pi}(2(H_{ext} + H_{uni}) + M_s) + \Delta f_{ex} \quad (3)$$

Where, Δf_{ex} implies the extrinsic line-width contributions. Therefore, the slope of Δf versus H_{ext} plot gives $\alpha(\gamma\mu_0/\pi)$ which is shown clearly in Fig. 6. We find that the slopes of each linear fitting line for d_x (= 10, 8, and 5 nm) are 1.51 ± 0.02, 1.24 ± 0.02, and 1.28 ± 0.04. α is transformed from each slope, the values for d_x (= 10, 8, and 5 nm) are 0.0270 ± 0.0004, 0.0221 ± 0.0004, and 0.0229 ± 0.0007. This implies that our measurement system makes it possible to obtain α exactly even in ultra-thin 5-nm Py film. As such, our measurement system is well equiped to detect and analyze α in keeping with our demands. From these result, we can scarcely distinguish α. Although α, which is enhanced from the mechanism of the extra scattering, depends on surface roughness, the differences of the samples are insignificant because our series of sample have quite small roughnesses.

In conclusion, we performed VNA-FMR measurements to formalize a well-defined measurement procedure for the Cu/Py/Cu series. We showed that there must be a careful process to analyze the Gilbert damping parameter obtained from the FMR-spectra. We believe that this measurement procedure will be helpful in eliminating background noise, enhancing the FMR-spectra signal from magnetic thin films of thicknesses below 10 nm (about 5 nm) while having a good resolution signal to noise ratio, and being able to analyze the damping parameter in magnetic thin film. This systematic accuracy must be used to study spin device's characteristics.

Acknowledgement

This work has been supported by the Research Grant of Kwangwoon University in 2010 and (2010-0022040 & 2010-0023798) through the NRF of Korea funded by MEST.

References

[1] J. F. Gantz, C. Chute, A. Manfrediz, S. Minton, D. Reinsel, W. Schlichting, and A. Toncheva, The Diverse and Exploding Digital Universe, An IDC white paper (2008) pp. 1-16.
[2] R. Beach, T. Min, C. Horng, Q. Chen, P. Sherman, S. Le, S. Young, K. Yang, H. Yu, X. Lu, W. Kula, T. Zhong, R. Xiao, A. Zhong, G. Liu, J. Kan, J. Yuan, J. Chen, R. Tong, J. Chien, T. Torng, D. Tang, P. Wang, M. Chen, S. Assefa, M. Qazi, J. DeBrosse, M. Gaidis, S. Kanakasabapathy, Y. Lu, J. Nowak, E. O'Sullivan, T. Maffitt, J. Z. Sun, and W. J. Gallagher Tech. Dig. IEDM 08-305 (2008).
[3] S. S. P. Parkin, U.S. Patent No. 6834005 (2004).
[4] S. S. P. Parkin, M. Hayashi, and L. Thomas, Science **320**, 190 (2008).
[5] S. Kaka, M. R. Pufall, W. H. Rippard, T. J. Silva, S. E. Russek, and J. A. Katine, Nature **437**, 389 (2005).
[6] C.-Y. You, J. Magn. Magn. Mater. **321**, 888 (2009); C.-Y. You, Appl. Phys. Lett. **92**, 192514 (2008); C.-Y. You, Appl. Phys. Lett. **92**, 152507 (2008).
[7] IEICE Tech. Rep. **109**, SDM2009-114, 91 (2009).
[8] C. Bilzer, PhD thesis, Universite Paris-Sud 11, France (2007).
[9] Anthony B. Kos, Thomas J. Silva, and Pavel Kabos, Rev. Sci. Instrum. **73**, 3563 (2002).
[10] M. B. An, D. Olligs, and C. Fermon, Phys. Rev. Lett. **91**, 137204 (2003).
[11] U. Ebels, L. D. Buda, K. Ounadjela, and P. E. Wigen, Spin Dynamics in Confined Magnetic Structures I, Springer, Berlin (2002) pp. 167-216.
[12] Y.-H. Shin, S.-S. Ha, D.-H. Kim, and C.-Y. You, J. Korean Magn. Soc. **20**, 18 (2010).
[13] D.-H. Kim and C.-Y. You, The Korean Physical Society 2010 Conference, Dp-I-012, Daejeon, April 21-23 (2010); D.-H. Kim and C.-Y. You, The Korean Magnetic Society 2010 Conference, S11, Wonju, June 10-12 (2010).
[14] http://www.cmicro.com/
[15] http://www.ggb.com/
[16] http://www.cmicro.com/products/calibration-tools/wincal-xe/wincal-xe-software1
[17] C. Bilzer, T. Devolder, P. Crozat, and C. Chappert, J. Appl. Phys. **101**, 074505 (2007).
[18] C. Bilzer, T. Devolder, P. Crozat, and C. Chappert, IEEE Trans. Magn. **44**, 3265 (2008).